www.czasopisma.pan.pl PAN www.journals.pan.pl
Chemical and Process Engineering 2015, 36 (1), 59-72
DOI: 10.1515/cpe-2015-0005

COMPUTATIONAL FLUID DYNAMICS AND EXPERIMENTAL STUDIES OF A NEW MIXING ELEMENT IN A STATIC MIXER AS A HEAT EXCHANGER

Maciej Konopacki[1], Marian Kordas[1], Karol Fijałkowski[2], Rafał Rakoczy[1*]

[1]West Pomeranian University of Technology, Szczecin, Institute of Chemical Engineering and Environmental Protection Processes, al. Piastów 42, 71-065 Szczecin, Poland

[2]West Pomeranian University of Technology, Szczecin, Faculty of Biotechnology and Animal Husbandry, Department of Immunology, Microbiology and Physiological Chemistry, al. Piastów 45, 70-311 Szczecin, Poland

The main aim of this work is to study the thermal efficiency of a new type of a static mixer and to analyse the flow and temperature patterns and heat transfer efficiency. The measurements were carried out for the static mixer equipped with a new mixing insert. The heat transfer enhancement was determined by measuring the temperature profiles on each side of the heating pipe as well as the temperature field inside the static mixer. All experiments were carried out with varying operating parameters for four liquids: water, glycerol, transformer oil and an aqueous solution of molasses. Numerical CFD simulations were carried out using the two-equation turbulence k-ω model, provided by ANSYS Workbench 14.5 software. The proposed CFD model was validated by comparing the predicted numerical results against experimental thermal database obtained from the investigations. Local and global convective heat transfer coefficients and Nusselt numbers were detrmined. The relationship between heat transfer process and hydrodynamics in the static mixer was also presented. Moreover, a comparison of the thermal performance between the tested static mixer and a conventional empty tube was carried out. The relative enhancement of heat transfer was characterised by the rate of relative heat transfer intensification.

Keywords: mixing, heat transfer process, static mixer, CFD, process intensification

1. INTRODUCTION

The use of the static mixer has been widely recommended for an important variety of applications, such as continuous mixing, heat and mass transfer processes and chemical reactions. Such mixers are designed to mix fluids without any recourse to the mechanical drive and static mixers may be used as an alternative to mechanical agitators. A motionless mixer is a specially designed geometrical structure of different shapes and forms of elements inserted in a long pipe. The number of elements and the type of a mixing device both depend on the mixing degree in any applications and a wide range of tasks. By using a specific geometrical combination of these elements one-after-another, the additional turbulence of the flowing fluid contributes to the improvement of mixing efficiency.

Static mixers have become standard equipment in the various branches of industry. These types of mixers are widely employed in-line in once-through processes. The benefits of the static mixer include low operating and maintenance costs, no mechanical seals, low energy consumption, it is self-cleaning and low shear forces prevent excessive stressing of the product (Ghanem et al., 2014). Nowadays, static

*Corresponding author, e-mail: rrakoczy@zut.edu.pl

mixers and their applications have become standard equipment in chemical, pharmaceutical, food processing, polymer synthesis, water treatment and petrochemical industries.

The static mixer may be used as a multifunctional heat exchanger in which mixing, chemical reaction and heat transfer can occur simultaneously in the same device. For a laminar flow in a plane pipe, thermal diffusion is the only heat transfer mechanism in the radial direction. The reduction of radial temperature gradients in fluids may be achieved by means of various types of motionless inserts. The effectiveness of static mixers to enhance heat transfer is due to their ability to promote radial flow and to bring fluid elements into close proximity so that diffusion or conduction becomes rapid. Motionless inserts change the hydrodynamics in fluids flowing inside tubes and the combination of effects can significantly increase heat transfer rates (Hirschberg et al., 2009; Jaworski and Pianko-Oprych, 2002; Perner-Nochta and Posten, 2007). Generally, static mixing elements can be used in either laminar or turbulent flow to improve heat transfer coefficients (Lisboa et al., 2010; Qi et al., 2003; Thakur et al., 2003).

Over the last 20 years and with the development of Computational Fluid Dynamics (CFD) and faster computers, it has become possible to analyse numerically hydrodynamics and heat transfer through a static mixer. Moreover, this technique can give access to qualitative and quantitative information concerning mixing performance through simply following particle trajectories, by examining concentrations or residence time distribution. CFD gives opportunities which are experimentally hard to achieve, like the determination of detailed flow and temperature profiles. Correlations based on numerical models may be helpful for design, optimisation and scale-up of process equipment (Abbasfard et al., 2014).

A considerable amount of literature has been published on the CFD modeling of the heat transfer process in various types of apparatus, such as: pipelines with different geometry and shape (Han et al., 2012; Jayakumar et al., 2010; Rosaguti et al., 2006; Schietekat et al., 2014; Zheng et al., 2013), heat exchangers (Afrianto et al., 2014; Freund and Kabelac, 2010; Yataghene et al., 2009), mechanical mixers (Delaplace et al., 2001; Kougoulos et al., 2005) or static mixers (Habchi and Harion, 2014; Solano et al., 2012; Wang et al., 2011). There are also some studies concerning CFD simulations of heat transfer in nanofluids (Fard et al., 2010; Utomo et al., 2012), objects inserted in fluid flow (Defraeye et al., 2010; Zare and Hashemabadi, 2013) or heat exchange enhancement (Eesa and Barigou, 2010; van Goethem and Jelsma, 2014).

CFD and numerical simulations may give access to qualitative and quantitative information concerning mixing performance or heat transfer enhancement in static mixers (Ghanem et al., 2014). The development of CFD models in recent years has contributed to the significant progress made in understanding of the thermal-hydraulics of heat exchangers (Jun and Puri, 2005). CFD technique is based on numerical methods that predict the governing transport mechanisms and it can be used to quantify many complex thermal-hydraulic phenomena (Norton et al., 2013). Generally, thermal processing heat transfer occurs due to one or more of three mechanisms: conduction, convection or radiation. Their fundamental representation is by means of differential equations. Heat transfer equations may be solved analytically for a small number of boundary and initial conditions. The application of numerical methods has allowed to work out these equations and build distributed parameter models that are also spatially and temporally representative of the tested system. Moreover, CFD codes allow to obtain solutions with a high level of physical realism. The ability of CFD to simulate numerically the flow and temperature distribution in a mixer can contribute significantly to the understanding of the mixing and heat transfer processes and to provide better, faster, and cheaper design optimisation (Lisboa et al., 2010). Relations based on CFD simulations would be helpful for scale-up process equipment and may be suitable for confirming a final design. Numerical studies are especially needed in the case of the exploration of new conceptual designs or the complicate geometry of insert (Ghanem et al., 2013; Meijer et al. 2012; Thakur et al. 2003).

In this work CFD is employed to study the heat transfer rate of the novel type of the static mixer for heating liquids and to analyse temperature patterns and heat transfer efficiency. The proposed CFD model is validated by comparing the predicted numerical results against experimental thermal database obtained from the investigations. Moreover, the obtained experimental and numerical results are compared with a conventional empty pipe heat exchanger with a similar heat transfer area.

2. EXPERIMENTAL

The static mixer experimental set-up for the investigations of the heat transfer process is presented in Fig.1.

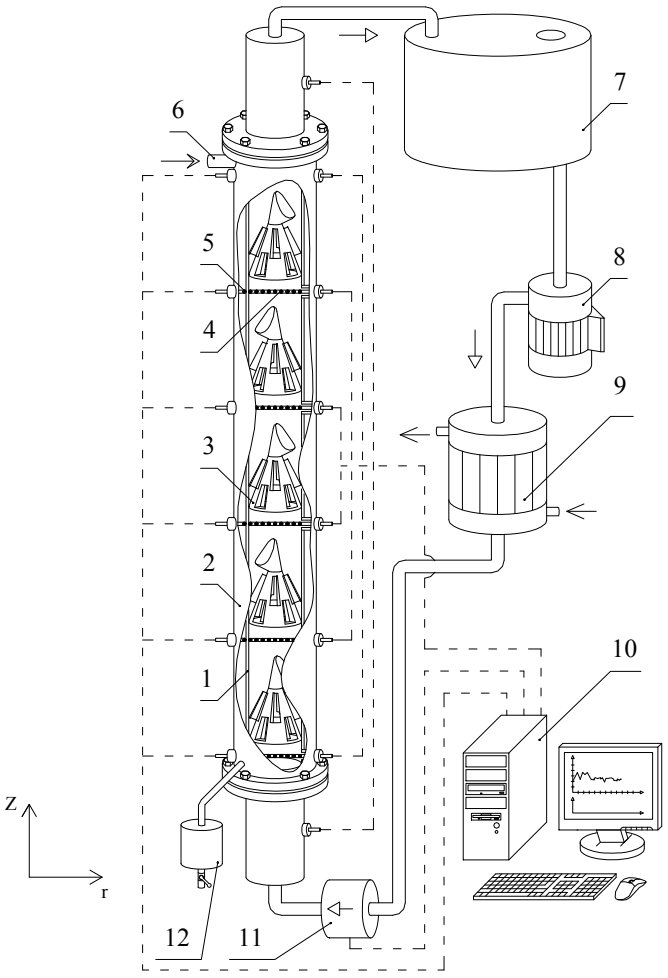

Fig. 1. The sketch of experimental set-up: 1 - wall, 2 - heat jacket, 3 - insert, 4 - internal temperature sensors, 5 - wall temperature sensor, 6 - steam inlet, 7 - buffer, 8 - circulation pump, 9 - heat exchanger, 10 - personal computer, 11 - flow meter, 12 - condensate outlet

This apparatus consists of an external heat exchanger, a circulating pump, an electrical steam generator and temperature sensors connected to digital measuring equipment. The heat from the condensing steam in the heating jacket was introduced to the flowing and mixed liquid by the novel mixing device.

The investigations were carried out with the static mixer equipped with a new mixing insert, which was a modified version of an mixer described in a patent registration (Masiuk and Szymański, 1997). The single mixing element had two truncated cones connected with each other. The diameter of the bigger cone was equal to the inner diameter of the apparatus. On the side surface of the inlet cone, longitudinal slots were placed symmetrically along the circumference. The slots were equipped with steering blades

placed on their longitudinal edges. The side surface of the inlet cone had an oval shape near its lower base. A stream of fluid flowing into the inlet cone was redistributed with the slots on the surface of the cone steering the flow outside, while the steering blades bestowed the arising streams with the rotational movement. A part of the stream leaving the inside of the insert through the outlet cone became turbulent due to the cone's oval shape. The inner and outer streams were mixed before entering the next mixing element where the streams were redistributed once again, rotated in the opposite direction, and reconnected. The novel mixing device was built from five separate segments in the form of two top opened cones. The large cone had longitudinal holes on the conical face with motionless outside baffles. The experiments were carried out with the cascade including 5 mixing elements.

The heat transfer enhancement was determined by measuring the profiles on each side of the heating pipe as well as the temperature field inside the static mixer. One system of temperature sensors was tightened closely to both sides of the inner tube and other bunches of small sensors were placed inside the bulk of the static mixer. The sensors were used to measure the distribution of the mixer bulk temperature across the radius and the length of the inner tube. The temperature within the mixed liquid varied significantly along the tube axis and increased much with the variation of the mass flow rate. Temperature variations in the cross section of the inner tube were measured and analysed.

The experimental set-up was equipped with a measuring instrument which controlled the temperature of the liquid and supervised the real-time acquisition of all the experimental data coming from the sensors. The device also measured temperature fluctuations inside the static mixer during the process. Electric signals were sampled by special thermal sensors (LM-61B, National Semiconductor Corporation, Santa Clara, USA) and were passed through the converter (PCI-1710HG, Advantech, Milpitas, USA) to a personal computer for further processing.

The experimental investigations were conducted for the steady-state condition of the heat transfer process. The measured temperature distribution was undertaken to determine the augmentation of the heat transfer by using the tested mixing device. As the fluids flowing through the inner pipe of the static mixer four liquids were used: water, glycerol, transformer oil and an queous solution of molasses. The mass flow rate was measured by means of an electromagnetic flow-meter. The experimental set-up with the thermal probes positions is shown in Fig. 2.

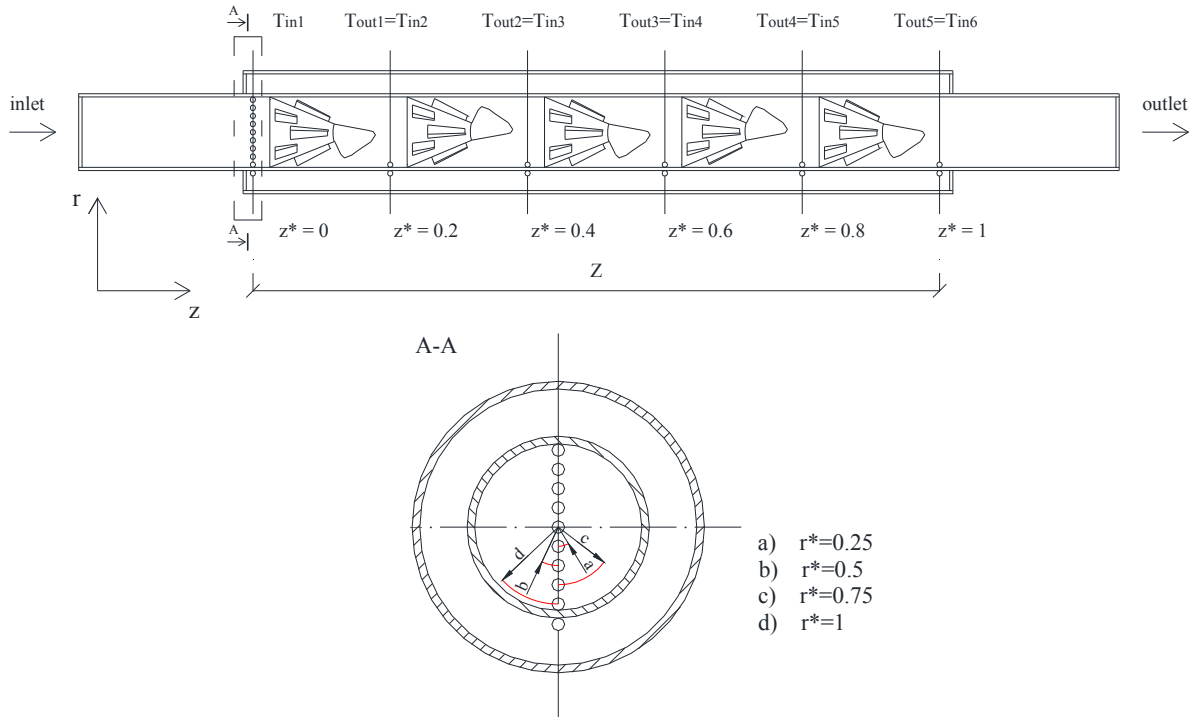

Fig. 2. The thermal probe positions in the experimental set-up

2.1. Numerical simulations

Numerical computations were carried out using the commercial CFD package ANSYS Workbench 14.5 (ANSYS, Inc., Canonsburg, USA). To calculate the liquid flow in the novel type of the static mixer, the geometry of the static mixer's inner tube (of the same dimensions as the real mixer) with five inserts by AutoCAD software (Autodesk, Inc., San Rafael, USA) was created. It is presented in Fig. 3.

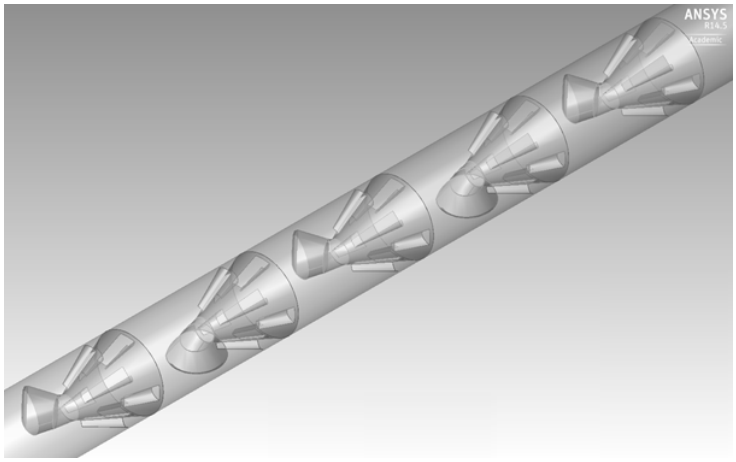

Fig. 3. View of geometry used in CFD simulations

The created geometry was imported to Design Modeler and introduced to ANSYS Meshing software to generate a CFD mesh. The numerical mesh consists of over 1.5 million triangular elements of acceptable quality. A large number of elements may help in obtaining more accurate results but also increases the time of the simulation. A mesh independence study was performed for grids containing 1.5, 2.5 and 3.5 million cells using the average temperature of fluid at the outlet of the static mixer (see Table 1). There were no significant differences between those grids and it was decided to do further computations on a 1.5 million cell grid. The numerical computations of fluid flow and heat transfer process was performed by means of ANSYS CFX software. This solver uses a control-volume formulation for solving the conservation equations of mass, momentum and energy. Each simulation was assumed to converge when the residuals for the energy equation were lower than 10^{-6} and those for equations of continuity and momentum were below 10^{-5}.

Table 1. Results of the mesh independence study

Number of cells (millions)	Average fluid temperature at outlet
1.5	345.43 K
2.5	345.44 K
3.5	345.45 K

The three-dimensional finite volume CFD code used in this study solves the steady, Reynolds-averaged Navier-Stokes (RANS) equations with the k-ω turbulence-closure model. This kind of numerical approach allows to compute complex laminar and turbulent flows in static mixers after applying appropriate corrections. The basic, two-equations k-ω model was proposed by Wilcox (Wilcox, 1988). Our variant of the model also contains modifications for low-Reynolds number effects, compressibility, and shear flow spreading.

The applied k-ω model may be used to analyse the flow inside the static mixer with a complex construction (Jones et al., 2002). In this case the predicted flow may be extremely complicated and

contains regions with a low level of turbulence or regions with local turbulence. Moreover, this particular model with automatic near-wall treatment automatically switches from wall-functions to a low-Reynolds near wall formulation. In addition, the *k-ω* model was validated extensively in complex, three-dimensional shear flows (Lin and Sotiropolous, 1997). It should be emphasised that the *k-ω* model is expected to be able to reasonably capture the characteristics of the laminar flow because the *ω*-equation possesses a solution as the turbulent kinetic energy approaches zero (Peng et al., 1996). The application of the *k-ω* model for low-Reynolds regions is presented in the relevant literature (Jones, 2000; Stringer et al., 2014; Togun et al., 2014).

3. RESULTS AND DISCUSSION

Data for liquid heating in the tested mixer was collected from the previous experimental investigations. Table 2 gives the ranges of the operating conditions and the calculated dimensionless numbers or ratios for the tested static mixing elements. All experiments were carried out systematically with varying operating parameters for four liquids: water, glycerol, transformer oil and an aqueous solution of molasses.

In the present work, temperatures are measured at different longitudinal positions and are used to compute local heat transfer coefficients. The coefficients are averaged over 5 incremental segments making up the total heat exchanger.

The convective heat transfer coefficient, α, in the dimensionless Nusselt number may be defined as the area-weighted harmonic mean of local heat transfer coefficient, α_z (Freund and Kabelac, 2010). Hobler (1986) defines the local heat transfer coefficient with the following equation:

$$\alpha_z = \frac{\pi D^2}{4}\frac{\dot{g}\, c_p}{F}\left(\frac{\Delta T_{in-out}}{\Delta T_{wall-bulk}}\right) \tag{1}$$

Having found the inlet liquid temperature in the static mixer, the average fluid temperatures at the inlet and outlet of each segment are computed by means of a simple energy balance between the heat transferred to the working liquid calculated for a given flow rate, specific heat and temperature gradient. The mean bulk and wall temperatures in each segment, $(T_{bulk})_{avg}$ and T_{wall} respectively, are used to determine α_z, the local heat transfer coefficient for each section:

$$(\alpha_z)_i = \frac{\pi D^2}{4}\frac{\dot{g}\, c_p}{F_i}\left(\frac{(T_{out})_i - (T_{in})_i}{(T_{wall})_i - \left[(T_{bulk})_{avg}\right]_i}\right) \tag{2}$$

The local Nusselt number, $(Nu_z)_i$, is then calculated, taking into consideration the following relation:

$$(\mathrm{Nu}_z)_i = \frac{(\alpha_z)_i D}{\lambda_{avg}} \tag{3}$$

A typical example of the spatial evolution of the local Nusselt number is plotted in Fig. 4 for different Reynolds numbers and for water used as the working liquid.

The increase in convective heat transfer along the novel type of the static mixer is explained by the development of the flow. The enhancement of the heat transfer process can be attributed to the breakdown of the thermal boundary layer, especially near the tube wall. It should be noticed that the enhancement is provided by the motionless mixer in which the higher heat flux or the heat transfer rate is achieved without the deterioration of the flowing fluid. Moreover, the increase in Reynolds number accentuates turbulent heat transfer and results in higher Nusselt numbers.

Table 2. The tabulated ranges of the operating conditions and the calculated dimensionless numbers

Type of fluid	$\dot{m}$ [kg s^{-1}]	ρ [kg m^{-3}]	c_p [J kg^{-1} K^{-1}]	λ [W m^{-1} K^{-1}]	μ [kg m^{-1} s^{-1}]
Water	0.04 - 0.28	980 - 988	4178 - 4187	0.649 - 0.665	$4.16\cdot10^{-4}$ - $4.16\cdot10^{-4}$
Glycelor	0.05 - 0.29	1202 - 1208	2586 - 1647	0.281 - 0.282	0.24 - 0.32
Transformer oil	0.04 - 0.25	835 - 842	2068 - 2125	0.121 - 0.122	$8.62\cdot10^{-3}$ - $1.08\cdot10^{-2}$
molasses (aqueous solution)	0.04 - 0.28	1272 - 1289	3440 - 3535	0.466 - 0.490	$2.70\cdot10^{-2}$ - $3.98\cdot10^{-2}$
Type of fluid	μ_w [kg m^{-1} s^{-1}]	μ / μ_w	$\dot{g}$ [kg m^{-2} s^{-1}]	w [m s^{-1}]	$\dot{V}$ [m^3 s^{-1}]
Water	$2.48\cdot10^{-4}$ - $5.19\cdot10^{-4}$	1.28 - 1.98	5.09 - 35.65	$5.17\cdot10^{-3}$ - $3.59\cdot10^{-2}$	$4.06\cdot10^{-5}$ - $2.82\cdot10^{-4}$
Glycelor	0.17 - 0.20	1.33 - 1.66	6.37 - 36.92	$5.28\cdot10^{-3}$ - $3.07\cdot10^{-2}$	$4.15\cdot10^{-5}$ - $2.41\cdot10^{-4}$
Transformer oil	$6.03\cdot10^{-3}$ - $7.59\cdot10^{-3}$	1.42 - 1.57	5.09 - 35.65	$6.08\cdot10^{-3}$ - $4.23\cdot10^{-2}$	$4.77\cdot10^{-5}$ - $3.32\cdot10^{-4}$
Molasses (aqueous solution)	$1.54\cdot10^{-2}$ - $2.70\cdot10^{-2}$	1.49 - 2.13	5.09 - 35.65	$3.98\cdot10^{-3}$ - $2.76\cdot10^{-2}$	$3.12\cdot10^{-5}$ - $2.17\cdot10^{-4}$
Type of fluid	Re	Pr	T_{in} [°C]	T_{out} [°C]	T_{wall} [°C]
Water	1037 - 5370	3 - 4	38.4 - 48.3	42.8 - 69.2	55.1 - 93.7
Glycelor	2 - 15	2272 - 2557	55.7 - 66.4	65.4 - 71.1	81.9 - 92.7
Transformer oil	54 - 330	163 - 183	52.7 - 53.8	56.5 - 67.3	73.0 - 92.7
Molasses (aqueous solution)	15 - 89	240 - 297	51.4 - 52.3	56.0 - 71.1	69.2 - 89.9
Type of fluid	T_{bulk} [°C]	$(T_{bulk})_{avg}$ [°C]	α [W m^{-2} K^{-1}]	Nu	
Water	38.8 - 66.8	40.6 - 58.2	276 - 1003	42 - 157	
Glycelor	56.8 - 70.5	62.9 - 68.7	159 - 543	56 - 192	
Transformer oil	53.2 - 66.3	54.7 - 61.0	95 - 342	78 - 280	
Molasses (aqueous solution)	51.8 - 69.2	53.7 - 61.8	266 - 807	56 - 174	

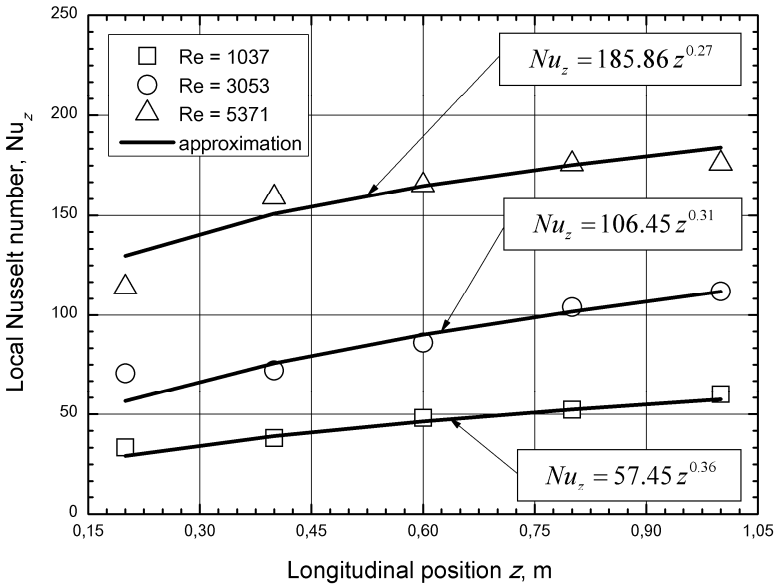

Fig. 4. Local Nusselt number for different Reynolds numbers (for water)

The thermal performance of the tested static mixer may be characterised by the global convective heat transfer coefficient, α_g, or the global Nusselt number, Nu_g, calculated using the area-weighted harmonic mean of the local heat transfer coefficients, $(\alpha_g)_i$.

In order to establish the effect of all important parameters on the heat transfer process in the tested set-up, in the widest range of variables, data obtained in the present work were analysed with the following relationship:

$$\mathrm{Re}^a\,\mathrm{Pr}^b\left(\frac{\mu}{\mu_w}\right)^c\left(\frac{D}{L}\right)^d \Rightarrow \mathrm{Nu}_g = A\,\mathrm{Pe}^a\left(\frac{\mu}{\mu_w}\right)^c\left(\frac{D}{L}\right)^d \Rightarrow \frac{\mathrm{Nu}_g}{\left(\frac{\mu}{\mu_w}\right)^c\left(\frac{D}{L}\right)^d} = A\,\mathrm{Pe}^a \tag{4}$$

The effect of heat transfer in the static mixer can be described using the variable $Nu_g\left(\frac{\mu}{\mu_w}\right)^{-c}\left(\frac{D}{L}\right)^{-d}$ proportional to the term $A\mathrm{Pe}^a$. The experimental results obtained in this work are graphically illustrated in $\log\left[Nu_g\left(\frac{\mu}{\mu_w}\right)^{-c}\left(\frac{D}{L}\right)^{-d}\right]$ versus $\log\left[A\,\mathrm{Pe}^a\right]$ in Fig. 5. The exponents of the rations (μ / μ_w) and (D / L) are 0.14 and 0.33 as there is some theoretical and experimental evidence for this value.

The proposed correlation (see Fig. 5) describes the global thermal behaviour of the tested static mixer flow over the range of Reynolds numbers studied and can be used as a design rule in the novel type of heat exchangers.

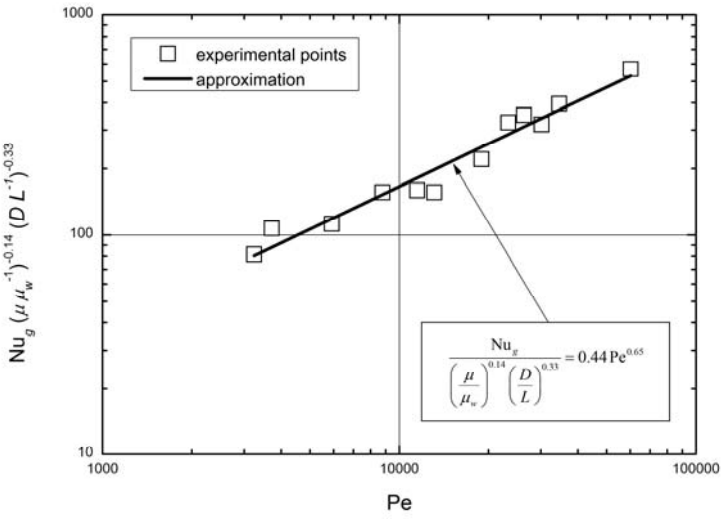

Fig. 5. The global Nusselt number as the function of the dimensionless Péclet number

A comparison of the thermal performance between the tested motionless inserts and a conventional empty tube was carried out. Hobler (1986) provides a correlation for the dimensionless Nusselt number in a straight plain pipe for $\left[\mathrm{Re}\,\mathrm{Pr}\left(\frac{D}{L}\right)\right] > 13$:

$$\mathrm{Nu}_p = 1.86\,\mathrm{Re}^{0.33}\,\mathrm{Pr}^{0.33}\left(\frac{\mu}{\mu_w}\right)^{0.14}\left(\frac{D}{L}\right)^{0.33} \Rightarrow \mathrm{Nu}_p = 1.86\,\mathrm{Pe}^{0.33}\left(\frac{\mu}{\mu_w}\right)^{0.14}\left(\frac{D}{L}\right)^{0.33}$$
$$\Rightarrow \frac{\mathrm{Nu}_p}{\left(\frac{\mu}{\mu_w}\right)^{0.14}\left(\frac{D}{L}\right)^{0.33}} = 1.86\,\mathrm{Pe}^{0.33} \tag{5}$$

The graphical comparison between the heat transfer rate for the tested static mixer and a straight plain pipe is illustrated in the plot given in Fig. 6.

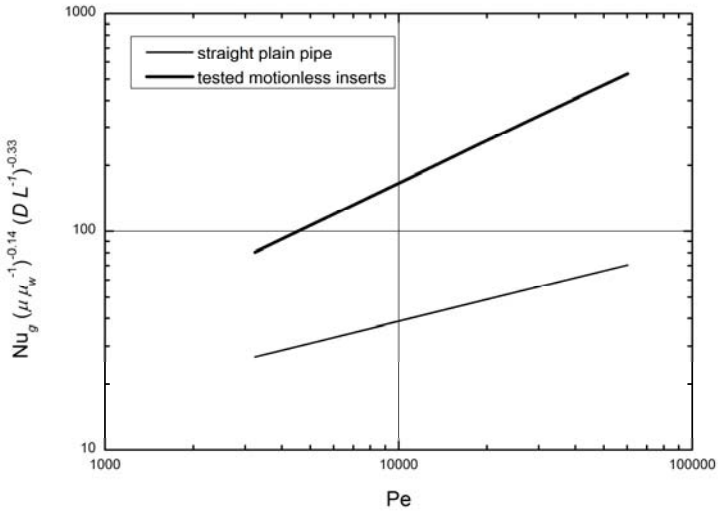

Fig. 6. A comparison of the obtained results for the tested static mixer and an empty pipe

Figure 6 shows that significant enhancement in the heat transfer performance for the applied static mixer is obtained with respect to the empty pipe. The obtained results indicate that the transfer rate for the tested static mixer is consequently higher than the data obtained for the heat transfer in the straight plain pipe.

To characterise this relative enhancement we define the rate of relative heat transfer intensification, κ, that reflects the increase in Nusselt number in the tested heat exchanger compared to a laminar tube flow. This factor is defined as follows:

$$\kappa = \frac{\mathrm{Nu}_g - \mathrm{Nu}_p}{\mathrm{Nu}_p} \tag{6}$$

Fig. 7 represents the relative intensification factor and suggests that the enhancement of heat transfer by the novel type of motionless inserts increases the Nusselt number by between 130% and 880% over that in a tube flow for the dimensionless Péclet numbers ranging between 3250 and 60300, respectively. The novel type of the static mixer produces considerable enhancement for the high Péclet number zone. This increase occurs because turbulent structures automatically start to appear in the static mixer that intensify convective transfer processes and deepen the sharp difference in Nusselt numbers in laminar regimes compared to the generated flow using the new type of motionless inserts.

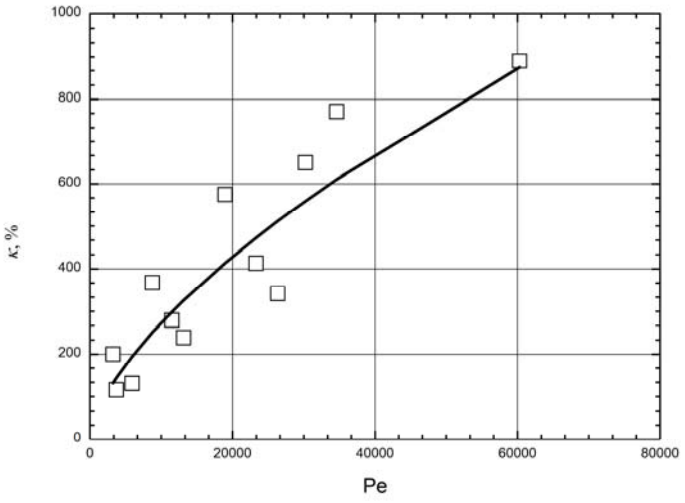

Fig. 7. A comparison of the obtained results for the tested static mixer and an empty pipe

The CFD model of the tested static mixer was validated by comparing the predicted results against experimental database presented in this paper. Fig. 8 shows a cross-sectional vertical cut along the central axial axis of the modelled static mixer, for the different operating conditions and water used as the working liquid.

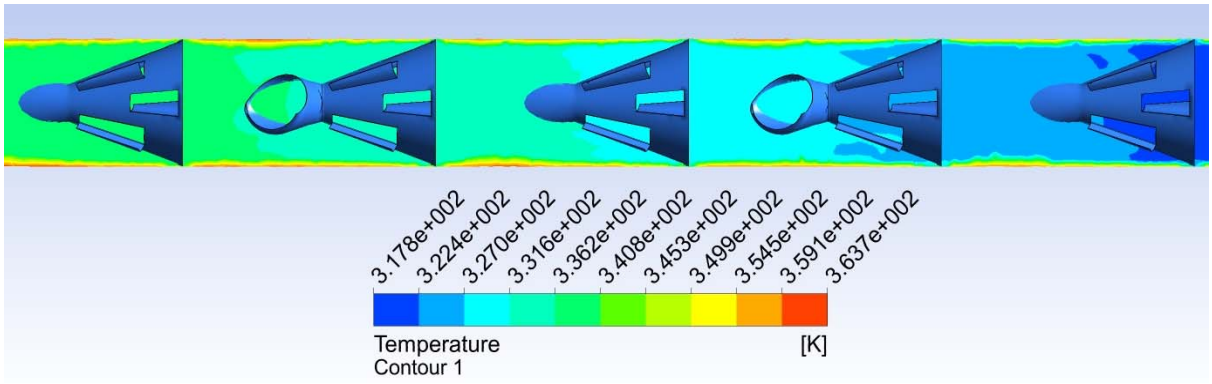

Fig. 8. The temperature contour generated by CFD modelling (water, $\dot{m}$ = 0.04 kg s^{-1})

As expected, the tested static mixer is able to reduce temperature gradients, thus producing a more uniform temperature distribution. The motionless elements direct the flow from the center towards the wall. This flow improves the radial mixing eliminating temperature gradients (see Fig.9).

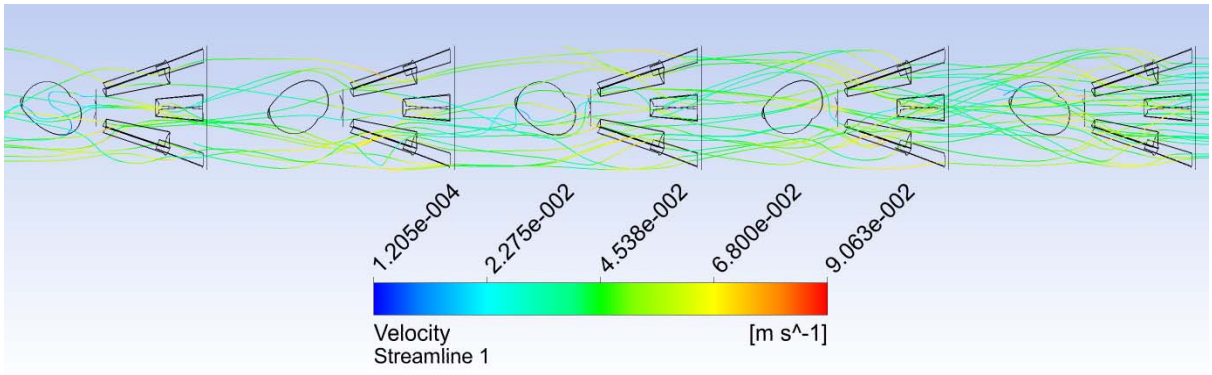

Fig. 9. The typical streamline of fluid velocity (water, $\dot{m}$ = 0.28 kg s^{-1})

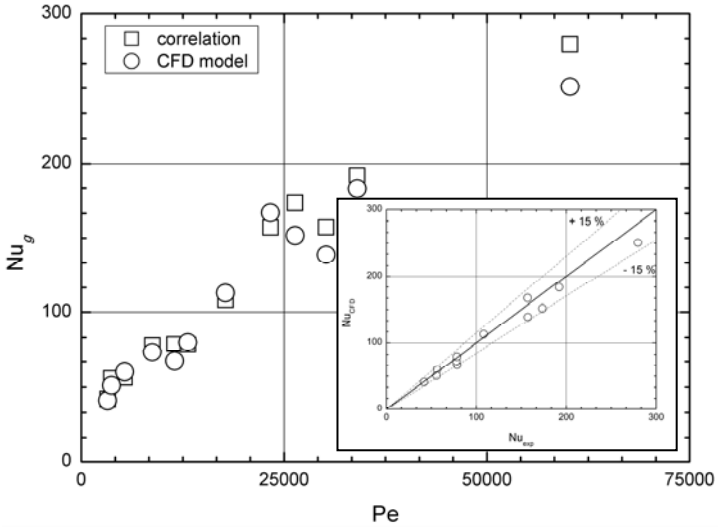

Fig. 10. Comparison of predicted (CFD model) and correlated (calculated values) global Nusselt numbers as the function of the dimensionless Péclet number

The CFD model was validated by comparing the obtained results against experimental thermal data. In Fig. 10 the estimated Nusselt numbers of the tested liquids are plotted against Péclet number. For purposes, the global Nusselt numbers calculated with the proposed experimental correlation (see Fig. 10) are also shown. Figure 10 shows that the numerically estimated Nusselt numbers are very similar to those calculated from the proposed experimental correlation. The numerical data are generally in good agreement with the correlation, exhibiting the same trend as the experimental data. The experimental values agree with the CFD model to within ±15%.

4. CONCLUSIONS

Several remarks resulting from the present investigations may be summarizsed as follows:

- The novel type of motionless mixer may be used as a heat exchanger in the laminar region of flow. In this case the tested static mixers can enhance heat transfer and provide more gentle product treatment that which can be achieved in empty or unpacked tubes.
- The description of the problem and the proposed relationships in the present paper is attractive because it generalises the experimental data of the heat transfer process taking into consideration the local heat transfer coefficients and the global Nusselt number.
- The values of the global Nusselt number in the tube equipped with the novel type of motionless inserts are higher than those in a plain tube (see Fig. 8).
- The forced convective heat transfer in the new type of static mixer was also modelled using CFD. The modified k-ω turbulent and thermal energy models were used to account for the heat transfer for the tested liquids and the operating conditions. The proposed numerical model was validated by comparing the predicted results against experimental database.

This work was supported by the Polish Ministry of Science and Higher Education from sources for science in the years 2012-2015 under Iuventus Plus project.

SYMBOLS

c_p	specific heat capacity, J kg^{-1} K^{-1}
D	inner diameter of mixer's tube, m (in the case of these results D = 0.1 m)
F	heat transfer area, m^2
F_i	heat transfer surface, m^2 (in our experiments $F_i = 0.2F = 0.2\pi DL$)
$\dot{g}$	mass flux, kg m^{-2} s^{-1}
i	number of section
k	turbulence kinetic energy, J kg^{-1}
L	length of static mixer's tube, m (in the case of these results L = 1 m)
$\dot{m}$	mass flow rate, kg s^{-1}
m	radial cylindrical coordinate (or radial position of the temperature sensor)
T	temperature, K
ΔT_{in-out}	the difference between the inlet temperature and outlet temperature;
$\Delta T_{wall-bulk}$	the difference between the wall temperature and the temperature of liquid inside the static mixer;

$\left[\left(T_{bulk}\right)_{avg}\right]_i$ averaged temperature inside static mixer's bulk for *i* section (in our experiments $\left[\left(T_{bulk}\right)_{avg}\right]_i = \frac{1}{m}\sum_{n=1}^{m}\left[\left(T_{in\ \text{or}\ out}\right)_m\right]_i$)

$\dot{V}$ volume flow rate. $m^3\ s^{-1}$

w linear velocity, $m\ s^{-1}$

z axial cylindrical coordinate

Greek symbols

α convective heat transfer coefficient, $W\ m^{-2}\ K^{-1}$

κ relative heat transfer intensification

λ thermal conductivity coefficient, $W\ m^{-1}\ K^{-1}$

μ fluid viscosity, $kg\ m^{-1}\ s^{-1}$

μ_w viscosity of fluid at wall's temperature, $kg\ m^{-1}\ s^{-1}$

ρ fluid density, $kg\ m^{-3}$

ω specific turbulence dissipation rate, s^{-1}

Subscripts

avg average value

bulk inside static mixer's bulk

g global value for static mixer

in inlet of static mixer

out outlet of static mixer

p empty pipe

wall wall of static mixer

z local value for static mixer

Dimensionless numbers

Nu Nusselt number

$(Nu_z)_i$, local Nusselt number,

Pr Prandtl number

Re Reynolds number

REFERENCES

Abbasfard H., Ghanbari M., Ghasemi A., Ghahraman G., Jokar S.M., Rahimpour M.R., 2014. CFD modelling of flow mal-distribution in an industrial ammonia oxidation reactor: A case study. *Appl. Therm. Eng.*, 67, 223-229. DOI: 10.1016/j.applthermaleng.2014.03.035.

Afrianto H., Tanshen R.M., Munkhbayar B., Suryo U.T., Chung H., Jeong H., 2014. A numerical investigation on LNG flow and heat transfer characteristic in heat exchanger. *Int. J. Heat Mass Transfer*, 68, 110–118. DOI: 10.1016/j.ijheatmasstransfer.2013.09.036.

Defraeye T., Blocken B., Carmeliet J., 2010. CFD analysis of convective heat transfer at the surfaces of a cube immersed in a turbulent boundary layer. *Int. J. Heat Mass Transfer*, 53, 297–308. DOI: 10.1016/j.ijheatmasstransfer.2009.09.029.

Delaplace G., Torrez C., Leuliet J.-C., Belaubre N., Andre C., 2001. Experimental and CFD simulation of heat transfer to highly viscous fluids in an agitated vessel equipped with a non standard helical ribbon impeller. *Chem. Eng. Res. Des.*, 79, 927–937. DOI: 10.1205/02638760152721460.

Eesa M., Barigou M., 2010. Enhancing radial temperature uniformity and boundary layer development in viscous Newtonian and non-Newtonian flow by transverse oscillations: A CFD study. *Chem. Eng. Sci.*, 65, 2199–2212. DOI: 10.1016/j.ces.2009.12.022.

Fard M.H., Esfahany M.N., Talaie M.R., 2010. Numerical study of convective heat transfer of nanofluids in a circular tube two-phase model versus single-phase model. *Int. Commun. Heat Mass Transfer*, 37, 91–97. DOI: 10.1016/j.icheatmasstransfer.2009.08.003.

Freund S., Kabelac S., 2010. Investigation of local heat transfer coefficients in plate heat exchangers with temperature oscillation IR thermography and CFD. *Int. J. Heat Mass Transfer*, 53, 3764–3781. DOI: 10.1016/j.ijheatmasstransfer.2010.04.027.

Ghanem A., Habchi Ch., Lemenand T., Della Valle D., Peerhossaini H., 2013. Energy efficiency in process industry – High efficiency vortex (HEV) multifunctional heat exchanger. *Renewable Energy,* 56, 96-104. DOI: 10.1016/j.renene.2012.09.024.

Ghanem A., Lemenand T., Della Valle D., Peerhossaini H., 2014. Static mixers: Mechanisms, applications,and characterization methods – A review. *Chem. Eng. Res. Des.*, 92, 205-228. DOI: 10.1016/j.cherd.2013.07.013.

Habchi C., Harion J.-C., 2014. Residence time distribution and heat transfer in circular pipe fitted with longitudinal rectangular wings. *Int. J. Heat Mass Transfer*, 74, 13–24. DOI: 10.1016/j.ijheatmasstransfer.2014.03.007.

Han H., Li B., Yu B., He Y., Li F., 2012. Numerical study of flow and heat transfer characteristics in outward convex corrugated tubes. *Int. J. Heat Mass Transfer*, 55, 7782–7802. DOI: 10.1016/j.ijheatmasstransfer.2012.08.007.

Hirschberg S., Koubek R., Moser F., Schöck J., 2009. An improvement of the Sulzer SMXTM static mixer significantly reducing the pressure drop. *Chem. Eng. Res. Des.*, 87, 524–532. DOI: 10.1016/j.cherd.2008.12.021.

Hobler T., 1986. *Heat transfer and heat exchangers*. Wydawnictwa Naukowo-Techniczne, Warszawa, Poland (in Polish).

Jaworski Z., Pianko-Oprych P., 2002. Two-phase laminar flow simulations in a Kenics static mixer. Standard Eulerian and Lagrangian approaches. *Chem. Eng. Res. Des.*, 80, 846-854. DOI: 10.1205/026387602321143462.

Jayakumar J.S., Mahajani S.M., Mandal J.C., Iyer K.N., Vijayan P.K., 2010. CFD analysis of single-phase flows inside helically coiled tubes. *Comput. Chem. Eng.*, 34, 430–446. DOI: 10.1016/j.compchemeng.2009.11.008.

Jones S.C., 2000. *Static mixers for water treatment: A computational fluid dynamics model*. PhD Thesis. Georgia Institute of Technology, Source DAI-B 61/04, p. 2132.

Jones S.C., Sotiropoulos F., Amirtharajah A., 2002. Nuemrical modeling of helical static mixers for water treatment. *J. Environ. Eng.*, 128, 431-440. DOI: 10.1061/(ASCE)0733-9372.

Jun S., Puri V.M., 2005. 3D milk-fouling model of plate heat exchangers using computational fluid dynamics. *Int. J. Dairy Technol.* 58, 214-224. DOI: 10.1111/j.1471-0307.2005.00213.x.

Kougoulos E., Jones A.G., Wood-Kaczmar M., 2005. CFD modelling of mixing and heat transfer in batch cooling crystallizers: Aiding the development of a hybrid predictive compartmental model. *Chem. Eng. Res. Des.*, 83, 30–39. DOI: 10.1205/cherd.04080.

Lin F.B., Sotiropoulos F., 1997. Strongly-coupled multigrid method for 3-D incompressible flows using near-wall turbulence closures. *J. Fluids Eng.*, 119, 314-324. DOI: 10.1115/1.2819136.

Lisboa P.F., Fernandes J., Simões P.C., Mota J.P.B., Saatdijian E., 2010. Computational-fluid-dynamics study of a Kenics static mixer as a heat exchanger for supercritical carbon dioxide. *J. Supercrit. Fluids*, 55, 107–115. DOI: 10.1016/j.supflu.2010.08.005.

Masiuk M., Szymański E., 1997. *Polish Patent No. 324,150*. Warszawa: Polish Patent and Trademark Office.

Meijer H.E.N., Singh M. K., Anderson P.D., 2012. On the performance of static mixers: A quantitative comparison. *Prog. Polym. Sci.*, 37, 1333-1349. DOI: 10.1016/j.progpolymsci.2011.12.004.

Norton T., Tiwari B., Da Sun W., 2013. Computational fluid dynamics in the design and analysis of thermal processes: A review of recent advances. *Crit. Rev. Food Sci. Nutr.*, 53, 251-275. DOI: 10.1080/10408398.2010.518256.

Paul E.L., Atiemo-Obeng V.A., Kresta S.M., 2004. *Handbook of Industrial Mixing*. Science and Practice, Wiley-Interscience, A John Wiley & Sons, Inc., Publication.

Peng S.H., Davidson L., Holmberg S., 1996. The two-equations turbulence *k*-ω model applied to recirculating ventilation flows. Rept. 96/13, Thermo and Fluid Dynamics, Chalmers University of Technology, Göteborg.

Perner-Nochta I., Posten C., 2007. Simulations of light intensity variation in photobioreactors. *J. Biotechnol.*, 131, 276–285. DOI: 10.1016/j.jbiotec.2007.05.024.

Qi Y., Kawaguchi Y., Christensen R.N., Zakin J.L., 2003. Enhancing heat transfer ability of drag reducing surfactant solutions with static mixers and honeycombs. *Int. J. Heat Mass Transfer*, 46, 5161–5173. DOI: 10.1016/S0017-9310(03)00221-7.

Rosaguti N.R., Fletcher D.F., Haynes B.S., 2006. Laminar flow and heat transfer in a periodic serpentine channel with semi-circular cross-section. *Int. J. Heat Mass Transfer*, 49, 2912–2923. DOI: 10.1016/j.ijheatmasstransfer.2006.02.015.

Schietekat C.M., van Goethem M.W.M., van Geem K.M., Marin G.B., 2014. Swirl flow tube reactor technology: An experimental and computational fluid dynamics study. *Chem. Eng. J.*, 238, 56–65. DOI: 10.1016/j.cej.2013.08.086.

Solano J.P., Herrero R., Espín S., Phan A.N., Harvey A.P., 2012. Numerical study of the flow pattern and heat transfer enhancement in oscillatory baffled reactors with helical coil inserts. *Chem. Eng. Res. Des.*, 90, 732–742. DOI: 10.1016/j.cherd.2012.03.017.

Stringer R. M., Zang J., Hillis A.J., 2014. Unsteady RANS computations of flow around a circular cylinder for a wide range of Reynolds numbers. *Ocean Eng.*, 87, 1-9. DOI: 10.1016/j.oceaneng.2014.04.017.

Thakur R.K., Vial C., Nigam K.D.P., Nauman E.B., Djelveh G., 2003. Static mixers in the process industries - A review. *Chem. Eng. Res. Des.*, 81, 787-826. DOI: 10.1205/026387603322302968.

Togun H., Safaei M.R., Sadri R., Kazi S.N., Baraduin A., Hooman K., Sadeghinezhad E., 2014. Numerical simulation of laminar to turbulent nanofluid flow and heat transfer over a backward-facing step. *Appl. Math. Comput.*, 239, 153-170. DOI :10.1016/j.amc.2014.04.051.

Utomo A.T., Poth H., Robbins P.T., Wacek A.W., 2012. Experimental and theoretical studies of thermal conductivity, viscosity and heat transfer coefficient of titania and alumina nanofluids. *Int. J. Heat Mass Transfer*, 55, 7772–7781. DOI: 10.1016/j.ijheatmasstransfer.2012.08.003.

van Goethem M.W.M., Jelsma E., 2014. Numerical and experimental study of enhanced heat transfer and pressure drop for high temperature applications. *Chem. Eng. Res. Des.*, 92, 663–671. DOI: 10.1016/j.cherd.2014.02.009.

Wang Y., Hou M., Deng X., Li L., Huang C., Huang H., Zhang G., Chen C., Huang W., 2011. Configuration optimization of regularly spaced short-length twisted tape in a circular tube to enhance turbulent heat transfer using CFD modeling. *Appl. Therm. Eng.*, 31, 1141-1149. DOI: 10.1016/j.applthermaleng.2010.12.009.

Wilcox D.C., 1988. Reassessment of the scale-determining equation for advanced turbulence models. *AIAA J.*, 26, 1299-1310. DOI: 10.2514/3.10041.

Yataghene M., Fayolle F., Legrand J., 2009. Experimental and numerical analysis of heat transfer including viscous dissipation in a scraped surface heat exchanger. *Chem. Eng. Process.*, 48, 1445–1456. DOI: 10.1016/j.cep.2009.07.012.

Zare M., Hashemabadi S.H., 2013. Experimental study and CFD simulation of wall effects on heat transfer of an extrudate multi-lobe particle. *Int. Commun. Heat Mass Transfer*, 43, 122-130. DOI: 10.1016/j.icheatmasstransfer.2013.02.010.

Zheng Z., Fletcher D.F., Haynes B.S., 2013. Chaotic advection in steady laminar heat transfer simulations: Periodic zigzag channels with square cross-sections. *Int. J. Heat Mass Transfer*, 57, 274–284. DOI: 10.1016/j.ijheatmasstransfer.2012.10.029.

Received 22 May 2014
Received in revised form 23 February 2015
Accepted 25 February 2015